

Antibacterial Activity, Structural, Optical And Morphological Properties Of Al Doped ZnO Nanoparticles Synthesized By Sol-Gel Method

C.Vijayaraj, G.Nedunchezian, S.Sozhaveni

Abstract: ZnO nanoparticles were synthesized by sol-gel method. The synthesized particles were characterized by XRD, SEM, EDAX, UV, FTIR and antibacterial studies. The X-ray diffraction studies reveals that the synthesized ZnO nanoparticles have wurtzite structure and the particle size varies from 10 to 26 nm. A change in morphology after doped with aluminium has been observed. The Energy Dispersive X-Ray Analysis (EDAX) reveals that the elemental composition of prepared samples and the incorporation of the Al ions into the ZnO lattice. The antibacterial activities of Al doped ZnO nanoparticles were examined using the disc diffusion method against four pathogenic bacteria (Escherichia Coli, Klebsiella Pneumoniae, Bacillus Cereus, and Staphylococcus aureus).

Keywords: Zinc Oxide, Nanoparticles, Antibacterial, XRD, UV, FTIR, SEM

1. INTRODUCTION

Zinc oxide play an vital role in industry, due to the efforts have been made to improve the properties of ZnO nanostructures by doping various chemical elements such as Ga [1, 2], In [3, 4], Sn [5], Mn [6], Mg [7], Bi [8] and Al [9, 10] into ZnO structures. Among them, Al-doped ZnO nanorods are capable of reaching the highest conductivity without deterioration in optical transmission and crystallinity and thus have been regarded as a potential alternative to the most accepted transparent conductive material [11]. Products such as flat panel displays, solar cells, optoelectronic and electronic components and thermally insulating architectural glass have one thing in common. Among many kinds of the metal oxide nanostructures that have been developed. Zinc oxide materials are having a variety of applications. Zinc oxide exhibits hexagonal wurtzite structure and has a direct band gap semiconductor around 3.37eV at 300K and the large exciton binding energy of 60 meV as an II-VI semiconductor [12-14]. Zinc oxide is a semiconductor used for various applications such as gas sensor, piezoelectric transducers and photo catalytic activity [15-16]. It has been synthesized with a variety of well defined nanostructures such as nanowires, nanorods, nanotubes and nanobelts [17-18]. The Al doped ZnO materials are most arguable. The ZnO is widely used in the gas sensors, solar cells, and luminescent, electrical and chemical sensors [19]. Among them, Al-doped ZnO nanoparticles are capable of reaching the highest conductivity without corrosion in optical transmission and crystalline and thus have been regarded as a potential alternative to the most accepted transparent conductive material. The products such as flat panel displays, solar cells, optoelectronic and electronic components and thermally insulating architectural glass have one thing in common. They have a combination of transparency and electrical conductivity. The quality of synthesis technique depends on its ability to control the important features of the nanocrystalline materials such as crystalline size and morphology of the nanoparticles. There

are many methods to synthesis ZnO nanomaterials namely, Solvo thermal method [20], Co-precipitation method [21], Hydro thermal method [22], Sol-gel method [23], Spray pyrolysis [24], and Vapour-liquid- solid method [25], so on. Among many techniques for preparing ZnO nanoparticles, sol-gel process has many advantages such as simple, inexpensive, and having large area applications. Aluminium has been an efficient n-type dopant to generate high quality samples with strong high transparency to visible light. Currently, biomedical nonmaterials have received more concern because of their well-known biological characteristic and biomedical applications. With the development of nanomaterials, metal oxide nanoparticles show promising and far-ranging prospect for biomedical field, mainly for antibacterial, anticancer drug delivery, cell imaging, biosensing and so on.[26] Pure cultures of all investigational bacteria and fungi were obtained from Microbial Type culture Collection Centre (MTCC), Chandigarh.

2 MATERIAL AND METHODS

The host precursor zinc acetate dihydrate ($\text{Zn}(\text{CH}_3\text{COO})_2 \cdot 2\text{H}_2\text{O}$) was dissolved in deionized water which was used as the starting solution (0.2 M). Aluminium nitrate (AlNO_3) was used dopant precursors for Al, respectively. The pH value of the starting solution was maintained at 9 by adding the required amount of NH_4OH solution. After, Tri-ethanolamine ($\text{C}_6\text{H}_{15}\text{NO}_3$) is added as surfactant to control size and morphology of nanoparticles. The resultant mixture was heated to 60 °C and magnetically stirred for 2hrs. After completed the stirring process the precipitate was separated carefully by filtration and washed several times with a mixture of ethanol and water kept in the ratio of 1:3. The final products were irradiated with microwave oven (LG India, frequency employing 2.45GHZ) for 30 min. Finally the powder calcined at 700 °C for 2hrs.

3. CHARACTERIZATION

Structural analysis was carried out using X-ray diffractometry (XRD) using $\text{CuK}\alpha$ radiation ($\lambda = 1.5406\text{\AA}$) in the 2θ range from 20° to 80°. Morphology and microstructure were identified by scanning electron microscope (SEM) and energy dispersive X-ray absorption (EDAX) respectively. The formation of ZnO wurtzite phase and available molecular bonds were investigated by the FTIR spectrum..The investigation of the

¹ PG & Research Department of Chemistry, Thiru. Vi. Ka. Govt. Arts College, Thiruvavur-610003.

² PG & Research Department of Physics, Thiru. Vi. Ka. Govt. Arts College, Thiruvavur-610003.

³ PG & Research Department of Physics, TBML College, Porayar-609307.

*Corresponding Author : cmvijaychem@gmail.com,

optical properties of these nanoparticles, the absorbance spectra of the samples were obtained using UV-vis-NIR spectrophotometer. The anti-bacterial and anti-fungal activities were examined for Al doped ZnO nanoparticles. Antibacterial and anti-fungal activities against two pathogenic bacteria and two pathogenic fungi were investigated by the agar disk diffusion method [27].

3.1. RESULTANT DISCUSSION

3.1.1 Structural study

The Fig.(3.1a) shows the X-ray diffraction (XRD) patterns of undoped and Al doped ZnO nanoparticles with different dopant concentrations of aluminum (Al³⁺). The structural properties of nanoparticles including crystalline size, lattice strain, dislocation density and crystalline orientation can be obtained from XRD spectra as represent Al doped ZnO nanopowder. The strong and clear peaks reveal the high purity and crystallinity of the as-prepared powder. The sharp diffraction peaks corresponding to (100), (002), (101) and (102) planes indicate the crystalline ZnO with hexagonal wurtzite structure, which are in close agreement with the standard card (JCPDS Code No. 36-1451). Besides the ZnO characteristic peaks, the peaks corresponding to (110) and (113) planes of AlNO₃ have also been detected (JCPDS Code No. 88-0826) [28]. The intensity of the peak (1 0 1) corresponding to AlNO₃ increases with increase of the Al content in the rod. From the spectra, broadening line clearly indicates synthesized powders in nanoscale. In figure (3.1) diffraction peaks at 31.20, 31.68°, 34.35°, 36.17°, 47.47°, 56.53°, 62.80°, 66.30°, 67.50°, 69.01°, 72.56°, 76.85°, 81.25°, 89.47°, 92.63°, 95.14° and 93.48° respectively. In particular, the intensity of diffraction peaks is enhanced significantly with increasing of Al³⁺ concentration. This behavior indicates that the increase in the doping concentration enhances the crystallinity, which may be attributed to the difference ionic radii of zinc, aluminum. With the increase of Al concentration, it has been reported that the intensity of diffraction peak decreased [29] The peaks confirm the formation of hexagonal wurtzite structure of ZnO nano powder (JCPDF 36-1451). The average crystallite size of nanopowders obtained using Scherrer's formula

$$D = \frac{0.9\lambda}{\beta \cos\theta}$$

Where D is grain size (nm), λ is wave length of the X-ray, β is FWHM, and θ is the Bragg angle.

where 'd_{hkl}' is interplanar distance and (hkl) are Miller indices the volume of the unit cell (v), the volume of the crystallites (V) and the number of unit cells in a crystallite (Nu) are calculated using the following relations:

$$v = \sqrt{3}2 a_2c 3$$

$$V = D^3 4$$

$$N 5 u = V/v$$

The estimated crystallite size and other structural parameters are given in Table (3.1). The calculated values of lattice parameters 'a' and 'c' and volume of the unit cell (v) do not deviate much from the standard JCPDS card values of ZnO. The mean crystallite size of the synthesized nanopowder increase with in Al doping concentration (from 24-26 nm) and increases [29].

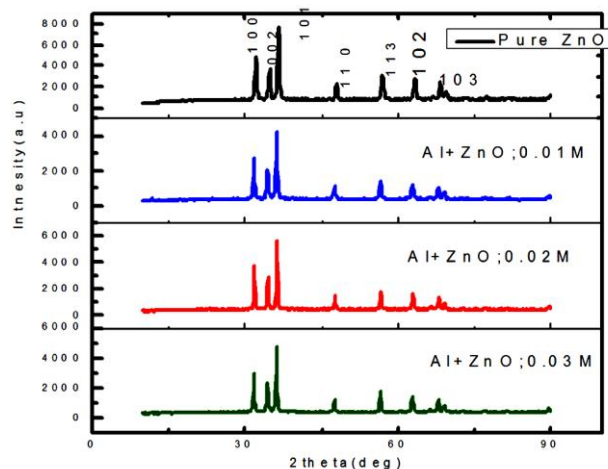


Fig.3.1 (a) XRD Spectra Analysis of Undoped Al doped ZnO Nanoparticles

In detail, the peak (101) of the Al doped ZnO nanoparticles shows a slight shift towards lower angle due to additional strain induced by the dopant in ZnO lattices as shown in Fig.3.1(b).

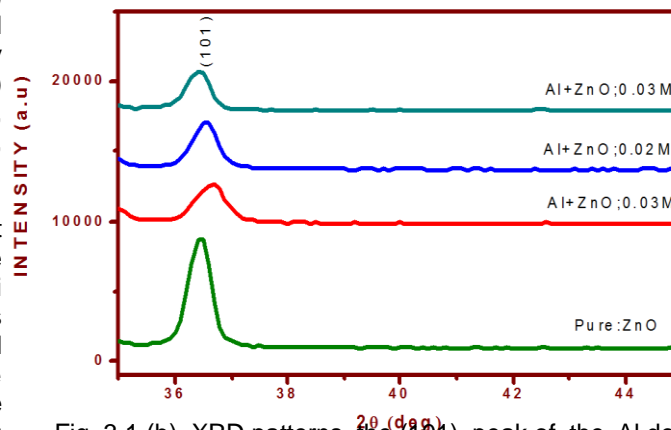


Fig. 3.1 (b). XRD patterns, the (101) peak of the Al doped ZnO nanoparicles.

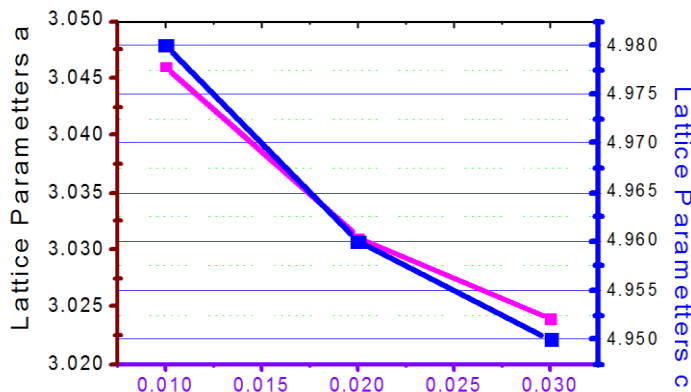


Fig. 3. 1(c). Lattice parameters 'a' and 'c' versus the concentration molarity

It is observed that as the molarity concentration increases, the lattice parameter 'a' decreases rapidly whereas the lattice parameter 'c' increases rapidly first and then starts decreasing. The plot of FWHM and grain size versus calcinations temperature is shown in Fig.3.1(c).

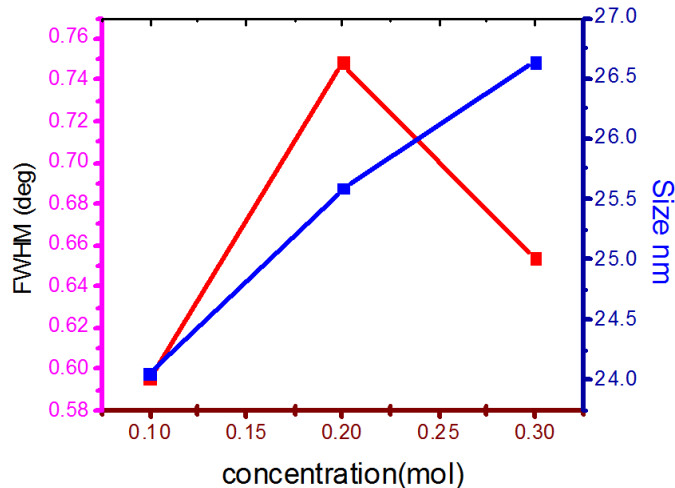


Fig.3.1(d). FWHM and Grain size versus molarity concentration.

The shift towards higher angle illustrates that Al ions have been successfully incorporated into the ZnO lattice and in turn decrease the lattice parameters a and c. The reaction temperature greatly influences the particle morphology of the as prepared ZnO powders and Al doped ZnO nanoparticles in various molarity 0.01, 0.02 and 0.03M. As the molarity concentration increases FWHM increases and at higher molarity concentration value FWHM decreases [30]. Thus the size of the Al doped ZnO nanoparticles shows variation as the concentration molarity increases as given in the Fig.3.1(d). The structural parameters of undoped and Al doped ZnO nanoparticles tabulated in Table 3. 1. The variation of the lattice parameters a and c with respect to the concentration molarity is as shown in Fig.3.1(c).

Table. 3.1 structural parameters of Undoped and Al doped ZnO Nanoparticles

| Sample | Molarity Ratio | Lattice Parameters (Å) | | | Grain size (D) nm | Dislocation density, $\delta \times 10^{-15}$ Lines/ m^2 | Strain, $\epsilon \times 10^{-3}$ | Volume, (Å) $\times 10^3$ |
|--------------|----------------|------------------------|-------|---------|-------------------|--|-----------------------------------|---------------------------|
| | | c (Å) | a (Å) | c/a (Å) | | | | |
| ZnO | Pure ZnO | 5.182 | 3.236 | 1.684 | 18.317 | 2.992 | 1.896 | 47.01 |
| Al doped ZnO | 0.1 M | 4.980 | 3.042 | 1.637 | 24.049 | 1.729 | 1.441 | 39.93 |
| Al doped ZnO | 0.2 M | 4.960 | 3.031 | 1.636 | 25.592 | 1.527 | 1.354 | 39.46 |
| Al doped ZnO | 0.3 M | 4.950 | 3.024 | 1.635 | 26.636 | 1.409 | 1.301 | 49.44 |

3.1.2 MORPHOLOGICAL ANALYSIS

3.1.3 SEM ANALYSIS

The SEM images of undoped ZnO and ZnO:Al nanopowders are shown in Fig.(3.3). The grain sizes of all the samples are in the nanoscale and have a rod like closely packed arrangement. It is seen that the grain size increase with the increasing doping concentration [31]. The increase in the grain size is one of the reasons for the enhancement in the antibacterial activities of the synthesized doped ZnO nanopowders as discussed in Sections Antibacterial studies.

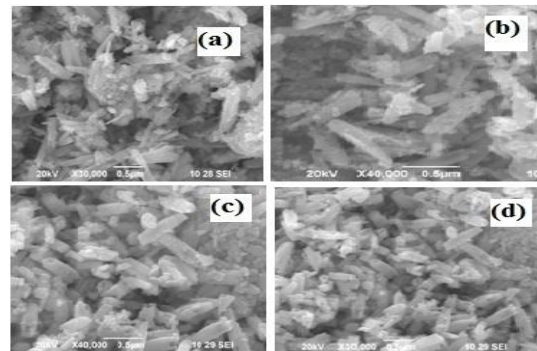


Fig.3.1.3 SEM Image of Al doped ZnO nanoparticles

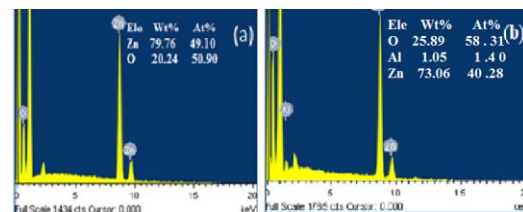


Fig.3.1.2 EDAX Analysis of Al doped ZnO Nanoparticles

The EDAX analysis indicates the successful undoped and aluminium doped ZnO nanoparticles which are with the coincidence of XRD result. The EDAX spectra of undoped and doped samples are shown in Fig.(3.2) Elemental analysis shows that the presents of elements Zn, Al, O are confirmed the Al doped ZnO nano particles. The Undoped ZnO contains only zinc and oxygen elements, where as the doped samples contains zinc, oxygen and aluminium in the appropriate ratios [32].

3.1.4 FTIR ANALYSIS

In the FT-IR spectra shown in Fig.(3.1.4) the broad absorption band at $\sim 3435 \text{ cm}^{-1}$ corresponds to the O-H stretching vibrations of water present in ZnO and the other transmission band at $\sim 3503 \text{ cm}^{-1}$ is assigned to a remaining organic component. The band at $\sim 1640 \text{ cm}^{-1}$ can be associated with the bending vibrations of H_2O molecules. The transmission band at $\sim 163 \text{ cm}^{-1}$ and $\sim 1383 \text{ cm}^{-1}$ in both the samples is due to the carbonyl groups of the carboxylate ions which might remain adsorbed on the surface of ZnO. The stretching of band appearing at 521 cm^{-1} confirms the formation of rod shaped ZnO particles [33]. The peaks appearing between 400 and 600 cm^{-1} are assigned to the metal-oxygen (M-O) stretching mode. Verges et al. already reported that appearance of peaks in three different positions depends on shapes of ZnO. The shape affects the position and intensity of

the peaks.

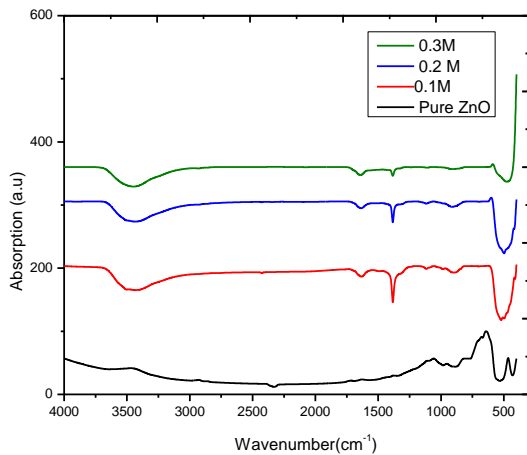


Fig.3.1.4 FTIR spectra of Al doped ZnO nanoparticles

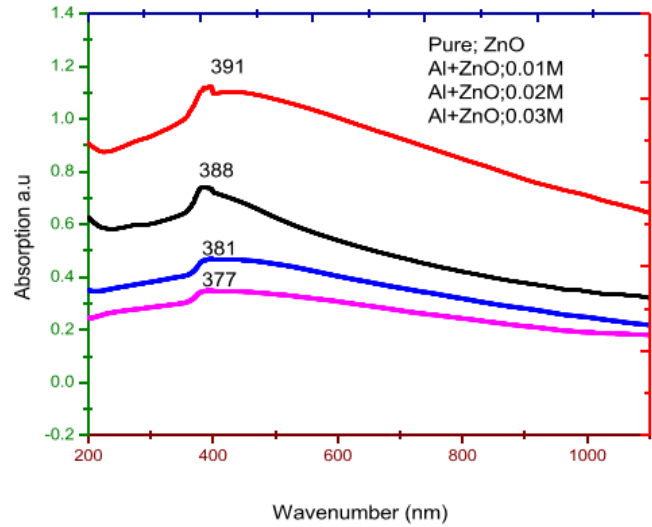


Fig.3.1.5a UV-VIS spectra of Al doped ZnO nanoparticles

3.1.5 UV-VIS ANALYSIS

Absorption of light by the semiconductor nanoparticles can be tailored by varying the energy band gap and the doping concentration. Fig. (3.1.5) shows absorption spectra of undoped and Al doped ZnO (0.01, 0.02 and 0.03%) respectively. The optical absorption spectra were recorded in the wavelength region of 300-800 nm. From these figures, it is clear that the absorption wavelength varies according to the change in doping concentration. The absorption edge shifts towards higher wavelength when the doping concentration increases. This indicates that the band gap of ZnO material decreases with the doping concentration upto some critical level which is known as Mott critical density. Above Mott critical density the absorption edge shifts towards the lower wavelength region. The lower wavelength shift or increase in the band gap or blue shift can be explained by the Burstein-Moss effect [34]. The Burstein-Moss effect is the process by which the apparent band gap of a semiconductor is increased as the absorption edge is pushed to higher energies as a result of all states close to the conduction band being populated. Increase in the dopant concentration leads to the supply of excess carriers which cause the increase band gap or blue shift. In Burstein-Moss effect the Fermi level merges into the conduction band with increase of doping concentration.

$$(\alpha hv)^{1/n} \sim (hv - E_g)$$

where α is the absorption coefficient, $h\nu$ is the photon energy, E_g is the optical band gap and n is the integer whose value depends on the nature of transition. Value of n is 1/2, 2, 3/2 and 3 for direct transition, indirect transition, forbidden direct transition and forbidden indirect transition respectively. The optical band gap was determined from the graph Fig. (3.1.5 a) 3. 1.5 b. The intercept of this plot on the energy axis gives the energy band gap of the samples. In this case ZnO, 0.01, 0.02 and 0.03M wt% Al doped ZnO shows the band gap of 3.38, 3.35, 3.28 and 3.17eV respectively tabulated in table 2.

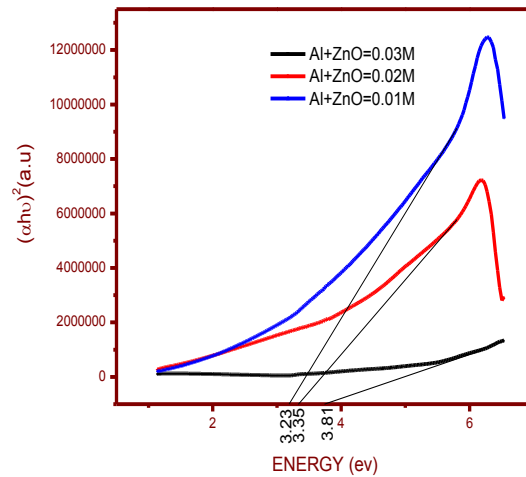


Fig 3.1.5(b): $(\alpha hv)^2$ vs (hv) spectra of Al -doped ZnO nanoparticles at various temperatures.

Table.3.2. Variation of absorption edges and energy band gap of Al doped ZnO nanoparticles at various molarity.

| Molarity | Absorption (nm) | Eg (E _v) |
|----------|-----------------|----------------------|
| ZnO | 391 | 3.17 |
| 0.01 | 388 | 3.28 |
| 0.02 | 381 | 3.35 |
| 0.03 | 377 | 3.38 |

ANTIBACTERIAL ACTIVITY

The synthesized Al doped ZnO nanoparticles of distinct shapes such nano rod like structures by the sol-gel process. The nanoparticles were subjected to annealing for 2 hrs at 700 C. The antimicrobial activity of Al doped ZnO nanoparticles were studied against two pathogenic bacteria strains, one Gram-positive (Staphylococcus aureus) and one Gram-negative (Escherichia coli) and two anti-fungal strains

(*Aspergillus flavus* and *Aspergillus niger*). Antibacterial and anti-fungal prospective Al doped ZnO nanoparticles were assed in terms of zone oh inhibition of bacterial growth [35-36]. The results of antibacterial and anti-fungal activities are presented in table 3.3.

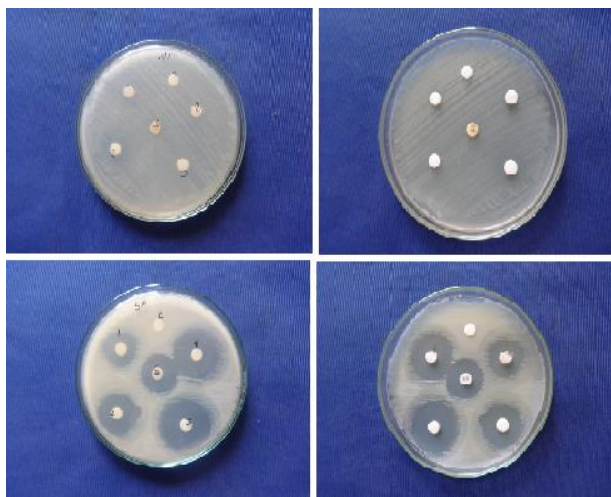


Fig.3.1.6 Antibacterial activity Al doped ZnO Nano particles

Table 3.3 Assay Of Antibacterial Activity

| S. No. | Bacteria | Zone of Inhibition (mm in diameter) | | | | | |
|--------|------------------------------|-------------------------------------|----|----|----|----|----|
| | | C | S* | 1 | 2 | 3 | 4 |
| 1 | <i>Escherichia coli</i> | - | 22 | 20 | 24 | 26 | 30 |
| 2 | <i>Staphylococcus aureus</i> | - | 20 | 18 | 20 | 24 | 26 |
| 3 | <i>Aspergillus flavus</i> | - | 10 | - | - | - | - |
| 4 | <i>Aspergillus niger</i> | - | 11 | - | - | - | - |

*Amikacin for Bacteria; Amphotericin b for Fungi

4. CONCLUSION

The Undoped and Aluminium doped ZnO nanoparticles were synthesized by sol-gel method. The effect of structural, morphological and optical properties of undoped and Al doped ZnO nanoparticles were investigated. The XRD analysis reveals that the prepared particles are in hexagonal wurtzite structure with an average particle size for undoped and doped ZnO nanoparticles less than 30 nm. The surface morphology analysis carried out using SEM and EDAX. The chemical groups of the samples were identified by FTIR spectra and prominent IR peaks were analyzed. UV-Vis measurement show free exciton absorption edges at 391, 388, 381 and 377 nm and a decrease in band gap of 3.17, 3.28, 3.35 and 3.38 eV with increase in molarity various. Thus, the current doping method can be regarded as one of the effective technique to modulate the optical properties of ZnO nanoparticles. The present study shows strong activity against the tested bacterial and fungal strains. The results were compared with standard antibiotic drugs. In this work Al doped ZnO nanoparticles were

found to be not inactive against any organism (Anti-bacterial) such as Gram-positive and Gram-negative and inactive for anti-fungal activities.

REFERENCE

- [1]. M. Yan, H.T. Zhang, E.J.Widjaja and R.P.H.Chang, Self-assembly of wellaligned gallium-doped zinc-oxide nanorods, *J. Appl. Phys.* 94 (2003) 5240
- [2]. Huihu Wang, Seonghoon Baek, Jaejin Song, Jonghyuck Lee and Sangwoo Lim, Microstructural and optical characteristics of solution-grown Ga-doped ZnO nanorod arrays, *Nanotechnology* 19 (2008) 075607.185
- [3]. Chao Liu, Haiping He, Luwei Sun, Qian Yang, Zhizhen Ye and Lanlan Chen, Acceptor-related emissions in indium-doped ZnO nanorods, *J. Appl. Phys.* 109 (2011) 053507.
- [4]. K.W.Liu, M.Sakurai and M.Aono, Indium-doped ZnO nanowires: Optical properties and room-temperature ferromagnetism, *J. Appl. Phys.* 108 (2010) 043516.
- [5]. Jahyun Yang, Juneyoung Lee, Kyungtaek Im and Sangwoo Lim, Influence of Sn doping in hydrothermal methods on the optical property of the ZnO nanorods, *physica E* 42 (2009) 51.
- [6]. Z.F. Wu, X.M.Wu, L.J.Zhung, B.Hong, X.M. Yang, X.M. Chen and Q.Chen, Synthesis and magnetic properties of Mn-doped ZnO nanorods via radiofrequency plasma deposition, *Mater.Lett.* 64 (2010) 472.
- [7]. Te-Hua Fang and Shao-Hui Kang, Preparation and characterisation of Mg-doped ZnO nanorods, *J. Alloy Compd.* 492 (2010) 536.
- [8]. Antonino Gulino and Ignazio Fragala, Deposition and Characterisation of Transparent Thin Films of Zinc Oxide Doped with Bi and Sb, *Chem.Mater.* 14(2002) 116.
- [9]. G.Srinivasan, R.T. Rajendra Kumar and J.Kumar, Influence of Al dopant on microstructure and optical properties of ZnO thin films prepared by sol-gel spin coating method, *Opt. Mater.* 30 (2007) 314.
- [10]. M.H. Mamat, Z.Khusaimi, M.F.Malek, M.Z.Musa and M.Rusop, Ultra-violetsensing characteristic and field emission properties of vertically aligned aluminium doped zinc oxide nanorod arrays, *AIP Conf.Proc.* 1341 (2011) 440.186
- [11]. Joon Hwan Lee, Chia-Yun Chou, Zhenxing Bi, Chen-Fng Tsai and Haiyan Wang, Growth-controlled surface roughness in Al-doped ZnO as transparent conducting oxide, *nanotechnology* 20 (2009) 395704.]
- [12]. M.Nirmala, Manjula G.Nair, K.Rekha, A.Amukaliani, S.K.Samdarshi and Ranjith G. Nair, Photocatalytic Activity of ZnO nanopowders Synthesized by DC Thermal Plasma, *African Journal of Basic & Applied Science* 2(5-6), 161-166, (2010)
- [13]. T.Khalid, Al-Rasoul, Nada K.Abbas, Zainb J. Shanan, Structural and Optical Characterization of Cu and Ni Doped ZnS Nanoparticles, *Int.J.Electrochem.Sci*, 8, 5594-5604, (2013)
- [14]. Zhigang Jia, Linhai Yue, Yifan Zheng, Zhude Xu, Rod-like Zinc Oxide constructed by nanoparticles Synthesis, characterization and Optical properties, *Materials Chemistry and Physics*, 107, 137-141, (2008)
- [15]. R. Saravanana, Kalavathy Santhia, N. Sivakumar, V. Narayanan, A. Stephen, Synthesis and characterization of ZnO and Ni doped ZnO nanorods by thermal decomposition method for

- spintronics application, *Materials Characterization*, 67 (2012) 10-16.
- [16] W.T. Wang, Z.H. Chen, G. Yang, D.Y. Guan, G.Z. Yang, Y.L. Zhou, H.B. Lu, Resonant absorption quenching and enhancement of optical nonlinearity in Au:BaTiO₃ composite films by adding Fe nanoclusters, *Appl. Phys. Lett.* 83 (2003) 1983–1985.
- [17] Linhua Xu a,n, XiangyinLi b a Influence of Fe-doping on the structural and optical properties of ZnO thin films prepared by sol–gel method *Journal of Crystal Growth* 312 (2010) 851–855.
- [18] Yang Liu, Ying Chu *, Likun Yang, Dongxue Han, Zhongxian Lu“A novel solution-phase route for the synthesis of crystalline silver nanowires, *Materials Research Bulletin* 40 (2005) 1796–1801.
- [19] U. O “zgu” r, Y.I. Alivov, C. Liu, A. Teke, M.A. Reshchikov, S.Dog’an, V. Avrutin, S.J. Cho, H. Morkoc,, A comprehensive review of ZnO materials and devices. *J. Appl. Phys.* 98, 041301 (2005)
- [20] Meenambika .R, Ramalingom .S And Chithambara Thanu .T Structural and Morphological Properties of Cr2O3 Nanoparticles Synthesized By Novel Solvent Free Method *Journal of Engineering Research and Applications* 4(2) 2014, pp.20-23
- [21] p. swapna1, s. venkatramana reddy1,a 0 structural and photoluminescence studies of (cu, al) co-doped zno nanoparticles mechanics, materials science & engineering april 2017 – issn 2412-5954doi 10.2412/mmse.77.36.550
- [22] A. Alkahlout,1,2 N. Al Dahoudi,1,2 I. Grobelsek,1 M. Jilavi,1 and P.W. de Oliveira1Synthesis and Characterization of Aluminum Doped Zinc Oxide Nanostructures via Hydrothermal Route*Journal of Materials* Volume 2014, Article ID 235638, 8 pageshttp://dx.doi.org/10.1155/2014/235638
- [23] A.Vanaja1, G. V. Ramaraju2 and K. Srinivasa Rao3 Structural and Optical Investigation of Al Doped ZnO Nanoparticles Synthesized by Sol-gel Process, *Indian Journal of Science and Technology*, Vol 9(12), DOI: 10.17485/ijst/2016/v9i12/87013, March 2016.
- [24] T.V. Vimalkumar, N. Poornima, K.B. Jinesh, C. Sudha Kartha and K.P. Vijayakumar, On single doping and Co-doping of spray pyrolysed ZnO films: Structural, electrical and optical characterization, *Appl.Surface Sci.* 257 (2011) 8334.
- [25] S. Mandal, H. Mullick, S. Majumdar, A. Dhar and S.K Ray, Effect of Al concentration in grain and grain boundary region of Al-doped ZnO films: adielectric approach, *J.Phys.D: Appl.Phys.* 41 (2008) 025307.
- [26]. P. K.Mishra, H. Mishra, A. Ekielski, S. Talegaonakar, and B. Vaidya, “ Zinc oxide nanoparticles: a promising nanomaterial for biomedical applications,” *Drug Discovery Today*, vol. 22, no. 12, pp.1825-1834, 2017.
- [27] A. B. Djuris'ic and Y. H. Leung, optical properties of ZnO nanostructures, *Small*.2 (2006) 944-961.
- [28] G. Muruganatham, K. Ravichandran, K. Saravanakumar, K.Swaminathan, N. J. Begum and B. Sakthivel: *Cryst. Res. Technol.*, 2012, 47, (4), 429–436.
- [29] V.Porkalai¹, B.Sathya¹, D.Benny Anburaj^{1*} G.Nedunchezhian¹, R.Meenambika Effect of Calcinations on the structure and morphological properties of Ag and In co-doped ZnO nanoparticles, *Journal of materials science and materials electronic*, 28(3), 2521-2528, (2017)
- [30] V Porkalai, D Benny Anburaj, B Sathya, G Nedunchezhian, R Meenambika, Study on the Synthesis, Structural, Optical and Electrical Properties of ZnO and Lanthanum Doped ZnO Nano Particles by Sol-Gel Method, *Mechanics, Materials Science & Engineering Journal*, Magnolithe, 2017, 9, . DOI 10.2412/mmse.77.37.393
- [31] B. Sathya¹ · D. Benny Anburaj¹ · V. Porkalai¹ · G. Nedunchezhian¹ Raman scattering and photoluminescence properties of Ag doped ZnO nano particles synthesized by sol–gel method *J. Mater Sci: Mater Electron* (2017) 28:6022–6032.
32. Lawrence Monah Ndam, Afui Mathias Mih,Aarom Suh Tening,Augustina Genla N wanaFongod,Nkegua AnnaTemenu and Yoshiharu Fujii,phytochemical analysis ,antimicrobial and anti oxidant activity of EuphorbiagolondrinaL.c.wheeler:an unexplored medicinal herb reported from Cameroon, *Journal of Springer Plus* (2016)5:264. DOI: 10.1186/s40064-016-1928-8.
- [33].R.S Zeferino, M.B. Flores and U.Pal, Photoluminescence and Raman scattering in Ag-doped ZnO nanoparticles, *J.Appl.Phys.* 109 (2011) 014308-1-014308-6
- [34]. Y.Jiang, L. Zhang, D. Wen and Y.Ding,“Role of physical and chemical interactions in the Antibacterial behavior of ZnO nanoparticles against E.coli,” *Material Science and Engineering: C*, vol.69, pp.1361-1366, 2016.
- [35]. Jinhuan Jiang, Jiang Pi, and Jiye Cai, The Advancing of Zinc Oxide Nanoparticles for Biomedical Applications. doi.org/10.1155/2018/1062562, 2018.
- [36]. T. C. Bharath, Shubham, S. Mondal, H.S.Gupta, P.K.Singh, A. K. Das, Synthesis of doped zinc oxide nanoparticles : A Reviw, *materials today, proceedings* 11, pp.767-775, 2019.